Three Isoforms of the Essential Translation Initiation Factor IF2 Differentially Modulate Homologous Recombination in *Escherichia coli*

Jillella Mallikarjun[1,2,3], L SaiSree[4], P Himabindu[1], K Anupama[1], Manjula Reddy[4], and J Gowrishankar[1,3]*

[1]Centre for DNA Fingerprinting and Diagnostics, Hyderabad 500039, India.

[2]Graduate Studies, Manipal Academy of Higher Education, Manipal 576104, India.

[3]Indian Institute of Science Education and Research Mohali, SAS Nagar 140306, India.

[4]CSIR-Centre for Cellular and Molecular Biology, Hyderabad 500007, India.

* To whom correspondence should be addressed: Prof J Gowrishankar (Orcid ID: 0000-0003-2483-9209), Tel: +91-172-2240266; Fax: +91-172-2240124; Email: shankar@iisermohali.ac.in

Abstract

In *Escherichia coli*, three isoforms of the essential translation initiation factor IF2 (IF2-1, IF2-2, and IF2-3) are generated from separate in-frame initiation codons in *infB*. The isoforms have earlier been suggested to act differentially in DNA replication restart. We report that in synthetic lethal situations associated with trapped Holliday junctions caused by deficiency of enzymes RuvAB or RuvC (that act in the post-synaptic step of homologous recombination [HR]), viability is restored in absence of any of the following: (i) IF2-1, (ii) RecA, which is the central protein for synapsis in HR, or (iii) proteins of the RecFORQ pre-synaptic HR pathway; conversely, loss of IF2-2 and IF2-3 exacerbated the synthetic defect. Strains lacking IF2-1 were also profoundly sensitive to two-ended DNA double-strand breaks (whose repair is mediated by RecA through the RecBCD pre-synaptic HR pathway), which was accompanied by reduction in extent of DNA loss around a break site. In HR assays, recovery of recombinants was diminished in IF2-1's absence. Our results suggest that isoforms IF2-1 and IF2-2/3 exert opposite effects at a step downstream of the two pre-synaptic pathways and of RecA nucleoprotein assembly, so as to increase and decrease, respectively, the efficiency of synapsis during HR.

Introduction

Genetically first identified as a mechanism to mediate exchange of hereditary determinants between cells (1), the process of homologous recombination (HR) in bacteria has also been recognized to play a crucially important role in maintenance of genomic integrity both during chromosomal replication and following DNA damage, just as is the case in archaea and eukaryotes [reviewed in (2–11)]. In *Escherichia coli*, protein RecA is central to the synaptic step of HR: RecA binds a suitable single-strand (ss)-DNA substrate to form a nucleoprotein filament that performs a homology search to enable annealing to a second suitable DNA molecule. This synaptic step is flanked by pre-synaptic and post-synaptic reactions, as described below.

The pre-synaptic reactions are designed to generate the ss-DNA substrate for RecA's binding. Two alternative pre-synaptic pathways RecBCD and RecFOR (named after the principal proteins mediating them) exist to prepare substrates from, respectively, double-strand breaks (DSBs) and ss-gaps in DNA. During DSB repair, RecBCD's exonuclease V (but not helicase) activity is modulated by cis site(s) in DNA designated Chi, which is an asymmetric 8-bp sequence. Loss of either RecBCD or RecFOR pathway alone affects certain categories of DNA recombination and repair, whereas combined loss of both pathways confers a deficiency as severe as that with loss of RecA itself (3, 8).

The presence of RecA-bound nucleoprotein serves also as a trigger for an SOS response within the cell, by which several prophages are induced to enter lytic growth and genes of the LexA-repressed SOS regulon are transcriptionally activated. For the SOS response, RecA's co-protease activity is stimulated following nucleoprotein assembly to facilitate auto-cleavage of LexA and prophage repressors [reviewed in (12)].

The post-synaptic reactions act to generate discrete recombinant DNA molecules following annealing of the DNA molecules and formation of Holliday junctions. The RuvAB helicase and RuvC resolvase are primary mediators at this step, which catalyze branch migration and resolution of Holliday junctions, respectively (3).

Included in the post-synaptic phase of HR are steps of replication restart, by which products generated after resolution of Holliday junctions are assimilated into the circular bacterial chromosome (or plasmid). Proteins mediating replication restart include PriABC, DnaT, and Rep, which are proposed to act through several alternative and redundant pathways that are designated as PriA-PriB, PriA-PriC, and Rep-PriC pathways; the Δ*priB* and *priA300* mutations have been suggested to specifically abrogate the PriA-PriB and PriA-PriC pathways, respectively [reviewed in (13–17)].

Studies of the past fifteen years from the Nakai group have identified an intriguing connection between translation initiation factor IF2 on the one hand and DNA transactions including DNA damage repair on the other (18–20). IF2 is a GTPase that participates in assembly of the 70S ribosome from its 30S and 50S subunits, in presence of mRNA, fMet-initiator tRNA and two other initiation factors IF1 and IF3, to initiate translation (21). It is essential for *E. coli* viability, and its function in translation initiation is conserved across bacteria, archaea, and eukaryotes (22, 23); a mammalian mitochondrial IF2 homolog can restore viability to an *E. coli* IF2 knockout strain (24). Three IF2 isoforms are synthesized in *E. coli* (see Supp. Fig. S2A), from in-frame initiation codons at positions 1,158, and 165 of the 890-codon-long *infB* ORF, that are herein designated as IF2-1, IF2-2 and IF2-3, respectively (25, 26). All isoforms are active for translation initiation and any one of them is sufficient for viability, since even a polypeptide with an artificial truncation of the N-terminal 388 amino acids of IF2 is able to support bacterial growth (27). Nevertheless, there is evidence that isoforms IF2-1 and IF2-2,3 (the latter designation is used for the mixture of IF2-2 and IF2-3, since they are only marginally different from one another) are together required for optimal growth of *E. coli* (28).

The Nakai lab has shown that IF2-1 and IF2-2,3 isoforms behave differently in vitro in assays for phage Mu transposition, and that they confer differential tolerance in vivo to genotoxic agents. They have proposed that the isoforms exert varying influences on different pathways of replication restart (18–

20). Relevant in this context is a report that IF2 is able to bind DNA through its C-terminal domain (29).

In this study, we have confirmed findings of the Nakai group (19, 20) that IF2-1 and IF2-2,3 isoforms are associated with differential effects on DNA damage repair. At the same time, our results indicate that these differential effects are exerted at an intermediate step in HR, which is downstream of both RecBCD and RecFOR pre-synaptic pathways and upstream of the post-synaptic steps of RuvABC action. In particular, we propose that it is the efficiency of RecA-mediated synapsis between a pair of DNA substrates that is diminished in absence of IF2-1.

Materials and Methods

Growth media, bacterial strains and plasmids. The routine rich and defined growth media were, respectively, LB and minimal A with 0.2% glucose (Glu) (30) and, unless otherwise indicated, the growth temperature was 37°. Supplementation with Xgal and with antibiotics ampicillin (Amp), chloramphenicol (Cm), kanamycin (Kan), spectinomycin (Sp), tetracycline (Tet), and trimethoprim (Tp) were at the concentrations described earlier (31). For induction of gene expression from the appropriate regulated promoters, L-arabinose (Ara), doxycycline (Dox), and isopropyl-β-D-thiogalactoside (IPTG) were added at 0.2%, 50 ng/ml, and 0.5 mM, respectively. Genotoxic agents were added at concentrations as indicated. *E. coli* strains used are listed in Supplementary Table S1, with the following knockout (Kan^R insertion-deletion) alleles sourced from the collection of Baba et al. (32): *dinF*, *dksA*, *greA*, *ilvA*, *leuA*, *leuD*, *racC*, *recA*, *recB*, *recO*, *recQ*, *recR*, *ruvA*, *serA*, *thrA*, *uvrD*, *ybfP*, and *yihF*; the Δ*infB* knockout mutation has also been described earlier (24).

Plasmids described earlier include pBR322 (Tet^R Amp^R, ColE1 replicon) (33); pACYC184 (Tet^R Cm^R, p15A replicon) (34); pCL1920 (Sp^R, pSC101 replicon) (35); pMU575 (Tp^R, single-copy-number vector with *lacZ*$^+$) (36); pHYD2411 (Tp^R, pMU575 derivative with *rho*$^+$) (37); and pTrc99A (Amp^R, for IPTG-inducible expression of gene of interest) (38). Plasmids pKD13 (Kan^R Amp^R), pKD46 (Amp^R),

and pCP20 (Cm^R Amp^R), for use in recombineering experiments and for Flp-mediated site-specific excision of FRT-flanked DNA segments, have been described by Datsenko and Wanner (39). Plasmids constructed in this study are described in the *Supplementary Text*.

Copy number analysis by deep sequencing after I-SceI cleavage. All cultures were grown in LB, and strains employed each carried an I-SceI site in *lacZ* and an Ara-inducible gene construct for I-SceI enzyme. Two alternative protocols were adopted to achieve I-SceI cleavage: Ara was added to a culture in early exponential phase and cells were then harvested after 60 min (40), or cultures were grown to mid-exponential phase in continuous presence of Ara. For each of the derivatives, a culture grown to mid-exponential phase in LB supplemented with Glu was used as the common (uninduced) control for either protocol. Copy number determinations of the various chromosomal regions were performed by a whole-genome sequencing (WGS) approach, essentially as described (41). Total DNA was extracted by the phenol-chloroform method, and paired-end deep sequencing was performed on an Illumina platform to achieve around 60- to 500-fold coverage for the different preparations. After alignment of sequence reads to the MG1655 reference sequence (Accession number NC_000913.3), gross read counts for non-overlapping 1-kb intervals were normalized to read counts per kb for a 600-kb region between genome co-ordinates 2501 and 3100 kb (which, relative to *oriC*, is "antipodal" to the region around *lacZ* on the opposite replichore, and is therefore expected to be the least affected following cleavage by I-SceI at *lacZ*). The moving average method for data smoothening was as described (41).

Other methods. Procedures were as described for P1 transduction (42), β-galactosidase assays (30), recombineering on the chromosome or plasmids (39), R-loop detection with S9.6 monoclonal antibody (43), and SbcCD-mediated cleavage of a palindromic site engineered in *lacZ* (44, 45). Protocols of Sambrook and Russell (46) were followed for recombinant DNA manipulations, PCR, and transformation. The Western blotting procedure, with rabbit polyclonal anti-IF2

or anti-Rho antisera (kind gifts from Umesh Varshney and Ranjan Sen, respectively), was essentially as described (47). Chromosomal integration, at the phage λ *att* site, of pTrc99A derivatives expressing IF2-2,3 or IF2-3, was achieved by the method of Boyd et al. (48). HR assay methods are described in the *Supplementary Text*, and include those based on conjugation (30), the Konrad assay (49), and inter-plasmid recombination (50, 51). Procedures for flow cytometric quantitation of dead cells by propidium iodide staining (52) are also described in the *Supplementary Text*.

Nomenclature for *infB* alleles. In the descriptions below, the designations *infB*$^+$ and Δ*infB* are used for the wild-type and deletion alleles, respectively, at the native chromosomal location. Nakai and coworkers (19, 20) have described the following set of three ectopic *infB* chromosomal constructs (designation used in this study for each of them given in parentheses): that encodes only IF2-1, but not IF2-2 or IF2-3 (Δ*2,3*); that encodes both IF2-2 and IF2-3, but not IF2-1 (Δ*1*); and that encodes all three isoforms (Δ*Nil*). The following P_{trc}-*infB* constructs were prepared in this work (designation used for each given in parentheses): that expresses both IF2-2 and IF2-3, but not IF2-1 (P_{trc}-Δ*1*); and that expresses IF2-3 alone (P_{trc}-Δ*1,2*).

Results

The genetic assays to identify lethality of mutants and their suppression. The genetic (blue-white) assay to demonstrate lethality has been described earlier (31, 37, 41). This method makes use of a single-copy-number-shelter plasmid encoding Tp^R and carrying *lacZ*$^+$ as well as a functional copy of the gene(s) of interest, and whose partitioning into daughter cells during cell division is not stringently regulated. Consequently, when a strain with this plasmid, along with Δ*lac* and a mutation in the gene of interest on the chromosome, is grown in medium not supplemented with Tp, plasmid-free cells that arise spontaneously in the culture (at around 5 to 20%) will be able to grow as white colonies on Xgal-supplemented plates if and only if the now unsheltered

chromosomal mutation is not lethal; on the other hand, control blue colonies (formed from cells retaining the shelter plasmid) would be observed as a majority in all situations. In the studies below, we have employed the blue-white assay with a shelter plasmid carrying either *rho*$^+$ or both *rho*$^+$ and *infB*$^+$ genes to examine lethality or synthetic lethality of *rho*, *rho-ruv*, and *infB* genes.

***rho-ruv* is synthetically lethal, suppressed by loss of IF2-1.** Rho is an essential protein in *E. coli* that mediates the termination of transcripts (other than rRNAs and tRNAs) which are not being simultaneously translated (37, 43, 53–56). Rho's function has been implicated in avoidance of RNA-DNA hybrids or R-loops (37, 43, 55, 57, 58), and maintenance of genomic integrity (59). A *rho* mutant was obtained with an *opal* (TGA) chain-terminating missense substitution in codon 136, which is viable in strains carrying the *E. coli* K-12 version of the *prfB* gene encoding release factor 2 (RF2) but not in those carrying the *E. coli* B version (Supp. Fig. S1A i-ii); there is evidence that the former but not the latter permits a low frequency of stop codon-readthrough (60). This was validated by Western blot analysis, which showed, for the *rho*-136^{opal} mutant, bands corresponding to both full-length (faint) and truncated Rho polypeptides (Supp. Fig. S1B). Another viable *opal* mutant in codon 157 of *rho* has been reported recently in *E. coli* K-12 (61).

The *rho*-136^{opal} mutation was synthetically lethal (on both rich and defined media) with disruptions of the *ruv* genes (Δ*ruvA*, Δ*ruvC*, or Δ*ruvABC*) encoding the Holliday junction enzymes RuvAB or RuvC (see, for example, Fig. 1A ii, and Supp. Figs. S3A i and S3B i). This *rho* mutation was not synthetic lethal with disruption of *recA* (Supp. Fig. S1A iii). One suppressor of *rho-ruv* lethality on both defined and rich media (Fig. 1A iii, and Supp. Fig. S3A ii) was mapped to the *infB-nusA* locus, and was shown by DNA sequencing to be an *ochre* (TAA) nonsense codon mutation at position 161 of the *infB* ORF. One would expect, from its location in the *infB* ORF, that this mutation abrogates synthesis of the IF2-1 and IF2-2 isoforms, which was confirmed by Western blotting (Supp. Fig. S2C, lane 6).

By itself, the *infB*-161^{ochre} mutation was lethal (Supp. Fig. S2B i) but it could be rescued by *rho* mutation (Supp. Fig. S2B ii). We interpret these findings as indicative of the notions (i) that nonsense substitution at codon 161 in *infB* induces Rho-mediated premature transcription termination within the gene, and therefore (ii) that synthesis of the lone IF2-3 isoform to ensure viability is itself contingent on relief of transcriptional polarity conferred by *rho* mutation.

Thus, viability of a triple mutant *rho ruv infB*-161^{ochre} is based on mutual suppression (i) of *infB*-161^{ochre} lethality by *rho*, and (ii) of *rho ruv* lethality by *infB*-161^{ochre}. This inference was supported by findings from experiments in which expression of an ectopically located *rho*$^{+}$ gene was placed under control of an Ara-inducible promoter (31) (Fig. 1B): that a *rho-ruv* derivative (row 3) is viable only on Ara-supplemented medium, whereas an *infB*-161^{ochre}-*rho* mutant (row 2) as well as the triple mutant *infB*-161^{ochre}-*rho-ruv* (row 4) are viable only on medium not supplemented with Ara. The *infB-rho* mutant was inhibited for growth at 22° (Supp. Fig. S2D), consistent with the known requirement for IF2 at low temperatures (62).

Based on the suppressor characterization results above, we tested two other sets of ectopic chromosomal *infB* constructs for their ability to rescue *rho-ruv* lethality, in derivatives carrying a deletion of the native *infB* locus. In one set of the ectopic constructs, which has been described earlier by Nakai and colleagues (19), IF2 expression remains under control of the natural *cis* regulatory elements for *infB* but not all isoforms are expressed from the different constructs (see Section on "Nomenclature for *infB* alleles" above; and see Supp. Fig. S2C, lanes 2 to 5 and lane 9 for correlations in Western blot analysis). Our results showed that the Δ*1* construct, but not Δ*2,3* or Δ*Nil*, could suppress *rho-ruv* synthetic lethality (Fig. 1A, compare vi with iv-v). This finding is consistent with that of *rho-ruv* suppression by *infB*-161^{ochre}, since the latter also fails to express isoform IF2-1.

The second set of ectopic chromosomal constructs P$_{trc}$-Δ*1* and P$_{trc}$-Δ*1,2*

(prepared in this study) were designed for differential expression of IF-2 isoforms from an IPTG-inducible heterologous P_{trc} promoter (see Supp. Fig. S2C, lanes 7-8, respectively, for Western blot confirmation). Both constructs could suppress *rho-ruv* lethality (Fig. 1A vii and Supp. Fig. S3B ii-iii), indicating once again that lethality suppression occurs when isoform IF2-1 is absent from the cells. Similar results were obtained irrespective of which *ruv* mutation (Δ*ruvA*, Δ*ruvC*, or Δ*ruvABC*) was used in the experiments (Fig. 1A iii, vi, vii; Supp. Fig. S3A, ii, v; and Supp. Fig. S3B ii-iii). With induced IF2-3 expression from the IPTG-regulated construct, suppression was obtained even in derivatives carrying the native *infB*$^+$ locus, but the colony growth was less robust (Fig. 1A viii).

These results indicate that it is an imbalance between levels of isoforms IF2-1 (low) and IF2-2,3 (high) that determines suppression of *rho-ruv* lethality. Loss of IF2-1 did not reverse the phenotypes associated with *rho* mutation (57), such as a Gal$^+$ phenotype that follows relief of premature transcription termination in the *gal* operon caused by *galEp3* mutation (Supp. Fig. S1C, compare iii-iv with ii), or lethality caused by runaway replication of plasmid pACYC184 (Supp. Fig. S1A iv-vi). Deficiency of IF2-1 did not also reverse UV-sensitivity known for *ruv* mutants (3, 63), and indeed it aggravated the phenotype (Supp. Fig. S2E). Thus, suppression of *rho-ruv* lethality by absence of IF2-1 is not because of restoration (or bypass) of Rho or Ruv function in these strains.

Loss of IF2-2,3 exacerbates *rho-ruv* defect. We expected that derivatives with the missense *rho-4* mutation (encoding Rho-A243E (57), see Supp. Fig. S1B lane 2 for Western blot) would be less compromised for Rho function than those with *rho*-136^{opal}, and a test for intracellular R-loop prevalence with monoclonal antibody S9.6 (43, 64) showed this to be so (Supp. Fig. S1D). Unlike *rho*-136^{opal}, the *rho-4* mutation was not synthetically lethal with *ruv* in the Nakai Δ*Nil* strain expressing all three IF2 isoforms (Fig. 1A ix). However, this combination (*rho-4 ruv*) conferred lethality in the Δ*2,3* derivative (lacking IF2-2,3) (Fig. 1A x), and this lethality was rescued by IPTG-induced expression of IF2-2,3 (Fig. 1A xi). Thus, absence of IF2-1 and of IF2-2,3 exert the apparently opposite phenotypes

of, respectively, alleviating and exacerbating the RecFORQ- and RecA-mediated sickness of *rho-ruv* mutants.

Loss of RecA, or of RecFOR pathway components, suppress *rho-ruv* lethality. Synthetic *rho-ruv* lethality was suppressed by the *rpoB*35* mutation (65–67) (Supp. Fig. S3A vii), as also by ectopic expression of the (phage T4-encoded) R-loop helicase UvsW but not its active site mutant version UvsW-K141R (68, 69) (Supp. Fig. S3A viii-ix). Both *rpoB*35* and UvsW alleviate the deleterious effects of Rho deficiency and can rescue Δ*rho* lethality (37, 43, 59). *rho-ruv* lethality was also rescued by Δ*recA* (Fig. 1C i, and Supp. Fig. S3A vi), raising the possibility that excessive (and unnecessary) HR triggered in presence of the *rho* mutation was leading to accumulation of Holliday junction intermediates in absence of RuvABC, resulting in cell death. The alternative explanation, that death was on account of excessive RecA-dependent SOS induction in *rho-ruv* mutants, was excluded since lethality was not rescued by the *lexA3* mutation [which encodes a LexA variant that is non-cleavable by RecA, and hence also abolishes SOS induction (12)] (Fig. 1C vi).

We then tested which of the two pre-synaptic pathways putatively feeds into the process of excessive HR in *rho-ruv* mutants. The synthetic lethality was suppressed by mutations in *recO* or *recR* (of the RecFOR pathway) (Fig. 1C ii-iii), but not by mutation in *recB* (of the RecBC pathway) (Fig. 1C iv). RecQ helicase activity is implicated in RecFOR pathway function (3, 8), and Δ*recQ* also was a suppressor of *rho-ruv* lethality (Fig. 1C v).

Synthetic lethality of *uvrD-ruv* is suppressed by loss of IF2-1. Several groups have earlier reported synthetic *uvrD-ruv* lethality (70–72), which is suppressed by *recA* and *recFORQ* but not *recBC* (that is, very similar to our findings with *rho-ruv* lethality). The mechanism invoked has been that of excessive and unnecessary HR in the *uvrD* mutant, leading to accumulation of toxic recombination intermediates in absence of RuvABC.

To test whether IF2 isoforms affect *uvrD-ruv* lethality, we expressed (from

a Dox-inducible promoter) a dominant-negative RuvC protein designated as RDG, that binds and traps Holliday junctions (63); these experiments were done in a set of Δ*uvrD* Δ*infB* derivatives each carrying one of the ectopically integrated Nakai constructs for different IF2 isoforms. Viability of the Δ*Nil* and Δ*2,3* strain derivatives was reduced 10^3- and 10^4-fold, respectively, upon Dox addition whereas the Δ*1* derivative was only minimally affected (Fig. 1D). A *recA* derivative of the Δ*Nil* strain survived Dox, as too did the control *uvrD*$^+$ *recA*$^+$ strain (Fig. 1D, last and first rows, respectively). These results confirm that *uvrD-ruv* is synthetically lethal (more severely so in absence of IF2-2,3), and that this lethality is rescued upon loss of RecA or of IF2-1.

Loss of IF2-1 confers profound sensitivity to two-ended DSBs in DNA. The Nakai group (19, 20) had shown previously that the Δ*1* strain expressing just the IF2-2,3 isoforms is sensitive to genotoxic agents such as methyl methanesulphonate or nitrofurazone, whereas the Δ*Nil* and Δ*2,3* strains are tolerant. In dilution-spotting assays, we confirmed the Nakai results for methyl methanesulphonate (Supp. Fig. S4A), and additionally found that the Δ*1* strain is profoundly sensitive to radiomimetic agents phleomycin (Phleo) or bleomycin (Bleo). Thus, at concentrations of Phleo or Bleo that provoke chromosomal two-ended DSBs (and so render a *recA* mutant inviable), the strain lacking IF2-1 was killed to at least the same extent as *recA* itself (Fig. 2A). On the other hand, the Δ*2,3*, *priA300* or Δ*priB* strains were as tolerant to these agents as was the Δ*Nil* strain (Fig. 2A). Phleo sensitivity of the Δ*1* strain could be complemented by plasmid-borne *infB*$^+$ (Supp. Fig. S4B). The Δ*1* strain (but not Δ*Nil* or Δ*2,3*), and a *recA* derivative of Δ*Nil*, were also markedly sensitive to two-ended DSBs generated by endonuclease I-SceI (Fig. 2B).

Sensitivity of the Δ*1* derivatives to Phleo or to I-SceI cleavage was demonstrated also by flow cytometry following propidium iodide staining for dead cells in cultures, wherein these strains exhibited much greater cell death than did the isogenic Δ*Nil* or Δ*2,3* strains (Fig. 2C, middle and bottom rows). Even in ordinarily grown cultures without any DNA damaging agent or treatment, around

8% of cells of the Δ*1* strain were scored as dead, a value comparable to that for *recA* and much higher than those for Δ*Nil* or Δ*2,3* derivatives (< 0.5% each) (Fig. 2C, top row); it should be noted, however, that these values do not take into account any contributions to inviability by anucleate cells or cell lysis in the cultures (73, 74).

It is the RecBCD pre-synaptic pathway that is involved in RecA-mediated recombinational repair of two-ended DSBs in DNA (3, 5–8), which was confirmed also in our experiments, by demonstrating that a *recB* but not *recO* mutant is sensitive to Phleo and Bleo (Supp. Fig. S4C). These results therefore establish that loss of IF2-1 is associated with compromise of two-ended DSB repair mediated by RecA and the RecBCD pre-synaptic pathway.

The results above were with perturbations generating two-ended DSBs in the genome. Interestingly, with lower concentrations of Phleo or Bleo wherein *recA* viability was only marginally affected, the strain without IF2-1 continued to exhibit marked sensitivity (Supp. Fig. S4D, compare rows 4 and 7 of three panels at left; supported also by data in Bleo sub-panel of Fig. 2A). This would suggest that at the low doses, DNA damage other than DSBs continues to occur (perhaps ss-DNA gaps), which can be repaired by RecA-independent mechanism(s) [such as by DNA polymerase I followed by DNA ligase (3)] but only so if IF2-1 is present.

On the other hand, the effect of IF2-1 loss on tolerance to some other perturbations or genotoxic agents that are also expected to generate DSBs was much less severe. Thus, type-2 DNA topoisomerase inhibitors nalidixic acid and ciprofloxacin were tolerated to equivalent extents by the strains with differential expression of the IF2 isoforms, but conferred 10^3-fold greater lethality upon loss of RecA or of PriB (Supp. Fig. S4A; see also Supp. Fig. S4C for sensitivity to ciprofloxacin of a *recB* but not *recO* mutant). The reversal in rank order of sensitivity between Δ*priB* and Δ*1* strains, to type-2 DNA topoisomerase inhibitors on the one hand and (high-dose) radiomimetic agents on the other, suggests that repair mechanisms following exposure to these two agent categories are distinct

and different, although both are RecA- and RecBCD-mediated (3, 75).

Again unlike a *recA* derivative, the Δ*1* strain was not sensitive to mitomycin C (Supp. Fig. S4A), nor was it killed upon DSB generation at a palindromic locus of a sister chromatid during DNA replication (44, 45) (Supp. Fig. S4E). The Nakai group (19) had previously shown that the Δ*1* strain is not sensitive to UV, which we have also confirmed (Supp. Fig. S2E, row 2).

Role of IF2 isoforms in two-ended DSB repair is independent of GreA/DksA. Loss of GreA (which binds within the secondary channel of RNA polymerase and restores it from a backtracked state during transcription elongation) is associated with increased tolerance to DSBs in DNA (40, 66, 67), which was confirmed for Phleo in this study (Supp. Fig. S4D, panel for 3 μg/ml). DksA is an apparent competitor to GreA with respect both to DSB repair (40, 66, 67) and to other phenomena (76, 77), and its loss conferred a modest sensitivity to Phleo (Supp. Fig. S4D, panels for 0.25 and 1 μg/ml).

Our results further show that sensitivity to Phleo of a strain lacking IF2-1 is reversed, but only partially so, upon loss of GreA and that it is somewhat exacerbated upon loss of DksA (Supp. Fig. S4D, panel for 0.25 μg/ml); thus the opposing effects of the two losses (IF2-1 and GreA) appear to be algebraically additive. These results suggest that the mechanism by which IF2-1 isoforms modulate DSB repair is different from that by GreA/DksA.

Genome-wide DNA copy number analysis following site-specific generation of a two-ended DSB. The Herman lab (40) has previously shown by WGS that following induction of synthesis of I-SceI to generate a two-ended DSB at a single genomic location in the *lac* operon, an equilibrium between DNA resection and re-synthesis is reached by 30 minutes wherein there is a Chi-site modulated, asymmetric V-shaped dip in DNA copy number extending from ~100 kb *ori*-proximal to ~200 kb *ori*-distal of the DSB site. The *recA* mutant, on the other hand, exhibits extensive ("reckless") DNA degradation.

We performed similar WGS experiments to determine genome-wide DNA copy numbers in LB-grown cultures for strains carrying an I-SceI site at the *lacZ* locus, and in which the cognate enzyme had been induced in early exponential phase for one hour (by addition of the inducer Ara); Glu was used instead of Ara in the control uninduced cultures. The strains carried the ectopic Nakai *infB* constructs (Δ*Nil*, Δ*1*, or Δ*2,3*) and were Δ*infB* at its native locus, and a *recA* derivative of the Δ*Nil* strain was also used (designated *recA* below).

Normalized copy number distributions from the cultures were determined as described above, and all of them exhibited a bidirectional *oriC*-to-*Ter* gradient that is expected for cells in asynchronous exponential growth in rich medium (Fig. 3). Superimposed upon this gradient distribution were several distinct features of interest, that are discussed separately below.

Following I-SceI induction with Ara, the Δ*Nil* strain and its *recA* derivative exhibited, respectively, the asymmetric V-shaped *Ter*-biased dip around *lacZ* (Fig. 3 v, and Supp. Fig. S5B i) and a very extensive degradation (Fig. 3 viii) as had previously been reported by the Herman group (40). The *recA* mutant also showed a small dip in *lacZ* region read counts in the Glu-grown culture (Fig. 3 iv and Supp. Fig. S5B, compare iv and v), suggestive of I-SceI cleavage in a minor proportion of cells even under uninduced conditions which is likely efficiently repaired in the IF2-1,2,3 strain but is lethal in *recA*.

Following 1-hr exposure to Ara, the Δ*2,3* strain behaved similarly to Δ*Nil* for copy number changes around *lacZ* (Fig. 3 vi and Supp. Fig. S5B ii), whereas the Δ*1* strain exhibited only a very minimal dip in read counts at this region (Fig. 3 vii and Supp. Fig. S5B iii). The latter finding was unexpected, since it was opposite to that in *recA* with which Δ*1* shares the phenotype of pronounced sensitivity to two-ended DSBs (including cleavage by I-SceI). The observation was reproducible, in that the Δ*1* strain cultured continuously with Ara also showed less or no dip in read counts around *lacZ* compared to that in the Δ*Nil* strain similarly cultured (Supp. Figs. S5A and S5B, compare, respectively, sub-panels

i with ii and vi with vii). Furthermore, we verified that the proportion of suppressors in the Δ*1* cultures (that is, survivors after Ara addition) was < 1%, nor did DNA sequence data for these cultures reveal mutations in any of the candidate genes related to DNA recombination and repair.

In the chromosomal terminus region, there was a peak of read counts between the *TerA* and *TerC/B* boundaries that was extremely prominent for the Ara-exposed cultures of Δ*Nil* and moderately so for Δ*2,3* and Δ*1* (Fig. 3A v-vii). As proposed earlier (78), we believe that this mid-terminus peak represents the algebraic sum of read counts of two major subpopulations, in which, respectively, clockwise and counterclockwise moving forks have traversed the terminus and are paused at Tus-bound *TerC/B* and *TerA*.

Another feature was the presence of sharp deep dips at several genomic positions (resembling stalactite images) which were especially pronounced in a Glu-grown culture of the Δ*1* strain, and representing $\log_2$ drops in normalized read counts of around 3 or more (Fig. 3 iii; and see maroon lines in Supp. Fig. S5C). Similar dips were observed in copy number curves for Glu-grown cultures of (in order of their prominence) *recA* and Δ*Nil* (Fig. 3 iv and i, respectively). The positions of these dips were identical in all three cultures, to a resolution of < 2 kb; five such representative genomic locations are depicted in Supplementary Figure S5C (green and violet lines for *recA* and Δ*Nil*, respectively). The dips were present also in Ara-exposed cultures of Δ*1* (Fig. 3 vii and Supp. Fig. S5A ii), and to less extent in those of *recA* and Δ*Nil* (Fig. 3 viii and Supp. Fig. S5A i, respectively). We suggest that this feature is correlated with presence in the strains of the gene encoding I-SceI, whose basal expression is perhaps associated with nickase activity (79) at specific sequences which then leads to ss-DNA gaps at these sites [since such ss-regions are not expected to be captured in Illumina WGS protocols (40)]. Indeed, dips at several of the identical locations were observed upon re-analysis of the Herman lab data (40) for uninduced cultures of wild-type and *recA* strains carrying the I-SceI gene, with those of *recA* being the more prominent (Supp. Fig. S5A iii-iv; and yellow and dark blue lines,

respectively, in Supp. Fig. S5C). Interestingly, the dips were least distinct for a Glu-grown culture of the Δ*2,3* strain (Fig. 3 ii, and light blue line in Supp. Fig. S5C); this last observation serves to exclude, as a possible explanation for these dips, sequence-specific bias in generation of read numbers during WGS.

To summarize, whole-genome copy number analysis in different strains without and with two-ended DSB generation at *lacZ* revealed the following: (i) after DSB generation, V-shaped dips in read counts around *lacZ* occur in Δ*Nil* and Δ*2,3* strains (more pronounced in former), that is associated also with peaks in the terminus region; (ii) *recA* exhibits extreme DNA degradation as expected under these conditions (40); (iii) on the other hand, the reduction of read counts around *lacZ* in the Δ*1* strain is minimal; and (iv) there are sharp dips in read counts at several genomic locations in uninduced cultures of the Δ*1* strain that are seen also in *recA* and Δ*Nil* but not so in Δ*2,3*.

HR frequency is oppositely affected by loss of IF2-1 and of IF2-2,3, and is elevated in *rho* mutants. To test the differential effects, if any, of IF2 isoforms on recovery of recombinants following HR, we employed several assays such as those of phage P1 transduction, inter-plasmidic recombination (that leads to reconstitution of Tet^R gene from two partially overlapping deletion alleles) (50, 51, 80, 81), and the Konrad assay (that similarly entails reconstitution of an intact *lacZ* gene from a split pair of partially overlapping *lacZ* fragments located at distant sites on the chromosome) (49, 82). Recombination events in each of the assays above are RecA-dependent (3, 49, 50); inter-plasmidic recombination is mediated by the RecFOR pre-synaptic pathway (50, 80, 81), whereas P1 transduction and recombination in the Konrad assay are RecBCD-dependent (49).

In the HR assays, loss of IF2-1 and of IF2-2,3 were associated with moderate reduction and elevation, respectively, in recovery of recombinants in comparison with values for the Δ*Nil* strain (Fig. 4A-C). A moderate reduction in P1 transduction frequency for the strain lacking IF2-1 has also been reported

earlier (19).

As expected (49, 82, 83), loss of UvrD conferred a hyper-recombination phenotype (Fig. 4A-B), but the HR frequency in a derivative that had lost both UvrD and IF2-1 was once again low and resembled that in a strain lacking IF2-1 alone (Fig. 4A, compare columns 3 and 6). Thus, loss of IF2-1 is epistatic to Δ*uvrD*, indicating that UvrD's function in HR precedes and is in the same pathway as that of IF2-1, but that the two act oppositely.

Since the results above suggested that loss of IF2-1 is associated with reduced RecA function in HR (see *Discussion*), we examined whether there is reduction in SOS induction [which is mediated by RecA's coprotease activity that is activated upon binding to ss-DNA (12)] as well in this situation. The results indicate that the basal SOS response, as measured by *sulA-lac* expression (84), is not decreased and may in fact be modestly elevated in the Δ*1* strain (Supp. Fig. S2F).

Our finding of *rho-ruv* synthetic lethality that is suppressed by *recA* suggests, based on its parallels with *uvrD-ruv* lethality, that non-essential HR occurs at elevated frequency in the *rho*-136^{opal} mutant. Measurements of HR frequency, both by the Konrad assay and by conjugation, indicate that the *rho* mutant does exhibit a moderate increase in HR frequency (Supp. Fig. S1E).

Discussion

The major findings of this study are those of (i) RecA- and RecFORQ-dependent *rho-ruv* synthetic lethality, and (ii) differential effects of IF2 isoforms on HR and DNA damage repair, and they are further discussed below.

Why is *rho-ruv* lethal? Several features are shared between synthetic lethalities *rho-ruv* and *uvrD-ruv*, suggesting commonality of mechanisms in the two instances. Thus, both lethalities require proteins RecA, RecFORQ, and translation initiation factor isoform IF2-1.

In case of *uvrD-ruv*, the model proposed by Rosenberg and colleagues (70) is that in absence of UvrD, there is excessive but unnecessary HR through the RecFORQ pathway, which then renders RuvABC essential for resolving the ensuing Holliday junction intermediates. Likewise for the *rho* mutant, we suggest that on account of an increased prevalence of R-loops with displaced ss-DNA, increased HR is triggered through the RecFOR pathway thus necessitating RuvABC's presence for viability; in this model, UvsW expression and *rpoB*35* are suppressors of *rho-ruv* lethality because they act to reduce R-loop prevalence in Rho-deficient strains (37, 43, 59). A recent study has shown that R-loops do stimulate HR in eukaryotic cells (85).

Opposing effects of IF2-1 and IF2-2,3 isoforms in HR pathways. Early studies had established that isoforms IF2-1 and IF2-2,3 are together required for optimal growth of *E. coli* (28). Nakai and coworkers (19, 20) have reported that loss of IF2-1 or of IF2-2,3 is each associated with sensitivity to different kinds of DNA damage.

In our study, loss of IF2-1 or of IF2-2,3 was associated with suppression or aggravation, respectively, of *rho-ruv* and *uvrD-ruv* sickness. The model for opposing effects of these isoforms is supported also by our findings in HR assays. At a mechanistic level, it is unclear whether a particular phenotype is caused by absence of one IF2 isoform or exclusive presence of another. An analogy can be drawn to the situation with DksA and GreA/B proteins, where too the effects of the loss of one protein can be mimicked by overexpression of the other (40, 76, 77).

How do IF2 isoforms influence HR and recombinational repair? Although our studies have identified IF2 isoforms as novel players in HR and recombinational repair, the mechanisms by which they act for this purpose are at present unknown. Loss of isoform IF2-1 phenocopies the partial or complete loss of RecA for at least four different phenomena: (i) suppression of *rho-ruv* and *uvrD-ruv* lethalities; (ii) profound sensitivity to two-ended DSBs in DNA provoked

by Phleo, Bleo, or I-SceI; (iii) presence of a significant proportion of dead cells in cultures during ordinary growth; and (iv) reduced recovery of recombinants following HR. Of these, at least the first and second involve, respectively, the RecFOR and RecBCD pre-synaptic pathways.

At the same time, DNA copy number analysis following I-SceI cleavage at *lacZ* has revealed that loss of RecA and of IF2-1 have opposite effects of decrease and increase, respectively, in copy number relative to values in the Δ*Nil* strain. For the strain lacking IF2-1, these data may point to either increased ("futile") repair synthesis or decreased degradation, relative to the parent. For example, repair synthesis is known to be increased in *recG* (44) or *recD* (45) mutants. Reduced DNA degradation at DSBs occurs in *greA* mutants (40), but in this case is correlated with enhanced tolerance to two-ended DSBs. An important unanswered question is identity of the exonuclease(s) responsible for DNA loss at a two-ended DSB site; although the degradation is Chi-site modulated in a wild-type strain, it nevertheless occurs (and indeed is substantially elevated) in a *recB* mutant lacking both helicase and exonuclease V activities of RecBCD (40).

Based on these features, we suggest that absence of IF2-1 leads directly or indirectly to reduction in efficiency of a step in HR which is (i) downstream of (and common to) the RecBCD and RecFOR pathways, and (ii) upstream of the post-synaptic reactions mediated by RuvABC. Formation of the RecA nucleoprotein is apparently unaffected, since the SOS response (12) is not perturbed by loss of IF2-1. Deficiency of IF2-2,3 is proposed to have the opposite effect of enhancing the efficiency of the same step in HR as that diminished by loss of IF2-1.

Thus, one possibility is that in absence of IF2-1, RecA nucleoprotein bundles are assembled which, however, are non-productive and inefficient in "homology searching" during the synaptic step of HR (11, 86); this notion is consistent with our finding that IF2-1's role in HR is downstream to that of UvrD, which acts to modulate efficiency of RecA nucleoprotein formation on DNA

564 substrates generated by the two alternative pre-synaptic pathways (83, 87). The
565 RecN protein, which is also required for DSB repair (88, 89), is postulated to act
566 at a step upstream of RecA-mediated synapsis (90); the epistatic relationship
567 between IF2 isoforms and RecN remains to be determined.

568 A requirement for homology searching may be more critical for certain
569 kinds of DNA damage such as two-ended DSBs than it is for others (89), which
570 could explain why loss of IF2-1 confers more sensitivity, relative to the Δ*Nil*
571 strain, to (high doses of) Phleo or Bleo than it does to mitomycin C or type-2 DNA
572 topoisomerase inhibitors. Even in other life forms, distinctive mechanisms exist
573 for two-ended DSB repair (91–95).

574 We further suggest that loss of IF2-1 leads to reduced exonuclease V action
575 (which is one component of RecBCD function) after DSBs are generated (3, 8,
576 11), resulting in reduced DNA degradation. Should this postulated second effect
577 of IF2-1 deficiency be in some way a consequence of the first, it may point to
578 existence of an interesting phenomenon of retrograde control of RecBCD
579 nuclease function by the RecA nucleoprotein filament, an idea that has
580 previously been suggested for *Caulobacter crescentus* (whose RecBCD equivalent
581 is AddAB) (96). The proposed second effect could also explain why loss of IF2-1
582 is associated with a log-scale decrease in efficiency of two-ended DSB repair
583 whereas its effects in the HR assays were more modest.

584 Our model that loss of IF2-1 compromises RecA function is different from
585 that of Nakai and colleagues (19, 20), who proposed that IF2 isoforms
586 differentially influence different replication restart pathways (which are post-
587 synaptic, and downstream of RuvABC action). As explained above, our finding
588 that loss of IF2-1 phenocopies the *recA* mutation in suppressing *rho-ruv* and
589 *uvrD-ruv* lethalities can best be explained only by invoking a role for IF2-1 prior
590 to the step of RuvABC action.

591 The other feature that distinguishes between IF2 isoforms is the set of
592 sharp dips in copy number read counts that occur at specific genomic locations

in strains with the I-SceI gene, even in uninduced cultures. On the assumption that the dips represent the net prevalence of ss-DNA gaps at these sites in cells of the population (that is, the balance between their generation and repair), it would appear that the magnitude of reduction in read counts (which is in the order Δ*1* > *recA* > Δ*Nil* > Δ*2,3*; Supp. Fig. S5C) inversely reflects the efficiency of their repair in the different strains. Consistent with this interpretation is our finding that loss of IF2-1 confers greater sensitivity than that of RecA to low concentrations of Phleo or Bleo (Supp. Fig. S4C), which may further suggest that in IF2-1's absence, RecA's non-productive binding to ss-DNA itself interferes with successful operation of the RecA-independent repair mechanisms.

To test the models above, in vitro studies are needed to examine whether IF2 isoforms act directly to modulate HR, and to determine their precise role(s) in the process. Regulation of HR and of recombinational repair functions is important in both prokaryotes and eukaryotes (97, 98), and factors previously identified for such regulation in *E. coli* include UvrD, mismatch repair proteins, DinI, and RecX (3, 83, 99–101).

Furthermore, IF2 would represent another example, apart from NusA (102–104) and GreA (40), of a protein earlier characterized for another critical function also participating in DNA repair. IF2 isoforms exist in other bacteria such as, for example, in species of the Gram-negative *Salmonella*, *Serratia* and *Proteus* (23) as well as in Gram-positive *Bacillus subtilis* (105), and their role if any in modulating HR may also be examined in future studies.

Data availability

The genome sequence and flow cytometry data described in this work are available for full public access from the repositories at http://www.ncbi.nlm.nih.gov/bioproject/734449 and https://flowrepository.org/id/FR-FCM-Z442, respectively.

Supplementary data

Supplementary data are provided in a PDF file "Supplementary data".

Funding

This work was supported by Government of India funds from (i) DBT Centre of Excellence (COE) project for Microbial Biology – Phase 2, (ii) SERB project CRG/ 2018/ 000348, and (iii) DBT project BT/ PR34340/ BRB/ 10/ 1815/ 2019. JM was recipient of a DST-INSPIRE fellowship, and JG was recipient of the J C Bose fellowship and INSA Senior Scientist award.

We declare that there are no conflicts of interest.

Acknowledgements

We thank R Harinarayanan, Hiroshi Nakai, Susan Rosenberg, Ranjan Sen, and Umesh Varshney for strains, plasmids, and reagents; Sayantan Goswami for recombineering of the I-SceI site in *lacZ*; Nalini Raghunathan and Apuratha Pandiyan for assistance with WGS data analysis; Anjana Badrinarayanan, Rachna Chaba, Dipak Dutta, and Mohan Joshi for comments on the manuscript; and COE team members for advice and discussions.

Author contributions: With the exception of the work components listed below, all experimental contributions in this study were by JM, under supervision of JG. LS, under supervision of MR, obtained and sequenced the *rho*-136^{opal} mutation, demonstrated *rho-ruv* lethality, and obtained and mapped a novel suppressor to the *nusA-infB* region. PH, under supervision of KA, determined the suppressor to be *infB*-161^{ochre}, performed the experiment for Fig. 1B, and constructed plasmid pHYD2906. JG drafted the manuscript.

References

1. Clark,A.J. (1973) Recombination deficient mutants of *E. coli* and other bacteria. *Annu. Rev. Genet.*, **7**, 67–86.

2. Kuzminov,A. (1995) Collapse and repair of replication forks in *Escherichia coli*. *Mol. Microbiol.*, **16**, 373–384.

3. Kuzminov,A. (1999) Recombinational repair of DNA damage in *Escherichia coli*

649 and bacteriophage λ. *Microbiol. Mol. Biol. Rev.*, **63**, 751–813.

650 4. Cox,M.M., Goodman,M.F., Kreuzer,K.N., Sherratt,D.J., Sandlerk,S.J. and
651 Marians,K.J. (2000) The importance of repairing stalled replication forks.
652 *Nature*, **404**, 37–41.

653 5. Sinha,A.K., Possoz,C. and Leach,D.R.F. (2020) The roles of bacterial DNA
654 double-strand break repair proteins in chromosomal DNA replication. *FEMS*
655 *Microbiol. Rev.*, **44**, 351–368.

656 6. Đermić,D. (2015) Double-strand break repair mechanisms in *Escherichia coli*:
657 recent insights. *Adv. Genomics Genet.*, **5**, 35-42.

658 7. Blackwood,J.K., Rzechorzek,N.J., Bray,S.M., Maman,J.D., Pellegrini,L. and
659 Robinson,N.P. (2013) End-resection at DNA double-strand breaks in the
660 three domains of life. *Biochem. Soc. Trans.*, **41**, 314–320.

661 8. Kowalczykowski,S.C. (2000) Initiation of genetic recombination and
662 recombination-dependent replication. *Trends Biochem. Sci.*, **25**, 156–165.

663 9. Lenhart,J.S., Schroeder,J.W., Walsh,B.W. and Simmons,L.A. (2012) DNA
664 repair and genome maintenance in *Bacillus subtilis*. *Microbiol. Mol. Biol. Rev.*,
665 **76**, 530–564.

666 10.Costes,A. and Lambert,S.A.E. (2013) Homologous recombination as a
667 replication fork escort: Fork-protection and recovery. *Biomolecules*, **3**, 39–
668 71.

669 11.Bianco,P.R. and Lu,Y. (2021) Single-molecule insight into stalled replication
670 fork rescue in *Escherichia coli*. *Nucleic Acids Res.*, **49**, 4220–4238.

671 12.Simmons,L.A., Foti,J.J., Cohen,S.E. and Walker,G.C. (2008) The SOS
672 Regulatory Network. *EcoSal Plus*, **3**, doi: 10.1128/ecosalplus.5.4.3.

673 13. Michel,B., Sinha,A.K. and Leach,D.R.F. (2018) Replication fork breakage and
674 restart in *Escherichia coli*. *Microbiol. Mol. Biol. Rev.*, **82**, e00013-18.

675 14. Gabbai,C.B. and Marians,K.J. (2010) Recruitment to stalled replication forks
676 of the PriA DNA helicase and replisome-loading activities is essential for
677 survival. *DNA Repair*, **9**, 202–209.

678 15. Michel,B. and Sandler,S.J. (2017) Replication restart in bacteria. *J.*
679 *Bacteriol.*, **199**, 1–13.

680 16. Heller,R.C. and Marians,K.J. (2006) Replisome assembly and the direct
681 restart of stalled replication forks. *Nat. Rev. Mol. Cell Biol.*, **7**, 932–943.

682 17. Huang,Y.H. and Huang,C.Y. (2014) Structural insight into the DNA-binding
683 mode of the primosomal proteins PriA, PriB, and DnaT. *Biomed Res. Int.*,
684 http://dx.doi.org/10.1155/2014/195162.

685 18. North,S.H., Kirtland,S.E. and Nakai,H. (2007) Translation factor IF2 at the
686 interface of transposition and replication by the PriA-PriC pathway. *Mol.*
687 *Microbiol.*, **66**, 1566–1578.

688 19. Madison,K.E., Abdelmeguid,M.R., Jones-Foster,E.N. and Nakai,H. (2012) A
689 new role for translation initiation factor 2 in maintaining genome integrity.
690 *PLoS Genet.*, **8**, e1002648.

691 20. Madison,K.E., Jones-Foster,E.N., Vogt,A., Kirtland Turner,S., North,S.H.
692 and Nakai,H. (2014) Stringent response processes suppress DNA damage
693 sensitivity caused by deficiency in full-length translation initiation factor 2
694 or PriA helicase. *Mol. Microbiol.*, **92**, 28–46.

695 21. Mechulam,Y., Blanquet,S. and Schmitt,E. (2013) Translation Initiation.
696 *EcoSal Plus*, **4**, doi: 10.1128/ecosalplus.4.2.2.

697 22. Lee,J.H., Choi,S.K., Roll-Mecak,A., Burley,S.K. and Dever,T.E. (1999)
698 Universal conservation in translation initiation revealed by human and
699 archaeal homologs of bacterial translation initiation factor IF2. *Proc. Natl.*
700 *Acad. Sci. U. S. A.*, **96**, 4342–4347.

701 23. Howe,J.G. and Hershey,J.W.B. (1984) The rate of evolutionary divergence of
702 initiation factors IF2 and IF3 in various bacterial species determined
703 quantitatively by immunoblotting. *Arch. Microbiol.*, **140**,187-192.

704 24. Gaur,R., Grasso,D., Datta,P.P., Krishna,P.D.V., Das,G., Spencer,A.,
705 Agrawal,R.K., Spremulli,L. and Varshney,U. (2008) A single mammalian
706 mitochondrial translation initiation factor functionally replaces two bacterial
707 factors. *Mol. Cell*, **29**, 180–190.

708 25. Plumbridge,J.A., Deville,F., Sacerdot,C., Petersen,H.U., Cenatiempo,Y.,
709 Cozzone,A., Grunberg-Manago,M. and Hershey,J.W. (1985) Two
710 translational initiation sites in the *infB* gene are used to express initiation
711 factor IF2 alpha and IF2 beta in *Escherichia coli*. *EMBO J.*, **4**, 223–229.

712 26. Nyengaard,N.R., Mortensen,K.K., Lassen,S.F., Hershey,J.W.B. and Sperling-
713 Petersen,H.U. (1991) Tandem translation of *E.coli* initiation factor IF2β:
714 Purification and characterization in vitro of two active forms. *Biochem.*
715 *Biophys. Res. Commun.*, **181**, 1572–1579.

716 27. Laalami,S., Putzer,H., Plumbridge,J.A. and Grunberg-Manago,M. (1991) A
717 severely truncated form of translational initiation factor 2 supports growth
718 of *Escherichia coli. J. Mol. Biol.*, **220**, 335–349.

719 28. Sacerdot,C., Vachon,G., Laalami,S., Morel-Deville,F., Cenatiempo,Y. and
720 Grunberg-Manago,M. (1992) Both forms of translational initiation factor IF2
721 (α and β) are required for maximal growth of *Escherichia coli*. Evidence for
722 two translational initiation codons for IF2β. *J. Mol. Biol.*, **225**, 67–80.

723 29. Vachon,G., Raingeaud,J., Dérijard,B., Julien,R. and Cenatiempo,Y. (1993)
724 Domain of *E. coli* translational initiation factor IF2 homologous to lambda *cI*
725 repressor and displaying DNA binding activity. *FEBS Lett.*, **321**, 241–246.

726 30. Miller,J.H. (1992) A Short Course in Bacterial Genetics: A Laboratory Manual
727 and Handbook for *Escherichia coli* and Related Bacteria. Cold Spring Harbor
728 Lab Press, New York.

729 31. Anupama,K., Leela,J.K. and Gowrishankar,J. (2011) Two pathways for
730 RNase E action in *Escherichia coli in vivo* and bypass of its essentiality in
731 mutants defective for Rho-dependent transcription termination. *Mol.*
732 *Microbiol.*, **82**, 1330–1348.

733 32. Baba,T., Ara,T., Hasegawa,M., Takai,Y., Okumura,Y., Baba,M.,
734 Datsenko,K.A., Tomita,M., Wanner,B.L. and Mori,H. (2006) Construction of
735 *Escherichia coli* K-12 in-frame, single-gene knockout mutants: The Keio
736 collection. *Mol. Syst. Biol.*, **2**, 2006.0008.

737 33. Bolivar,F., Rodriguez,R.L., Greene,P.J., Betlach,M.C., Heyneker,H.L.,
738 Boyer,H.W., Crosa,J.H. and Falkow,S. (1977) Construction and
739 characterization of new cloning vehicle. II. A multipurpose cloning system.
740 *Gene*, **2**, 95–113.

741 34. Chang,A.C.Y. and Cohen,S.N. (1978) Construction and characterization of
742 amplifiable multicopy DNA cloning vehicles derived from the P15A cryptic
743 miniplasmid. *J. Bacteriol.*, **134**, 1141–1156.

744 35. Lerner,C.G. and Inouye,M. (1990) Low copy number plasmids for regulated
745 low-level expression of cloned genes in *Escherichia coli* with blue/white
746 insert screening capability. *Nucleic Acids Res.*, **18**, 4631.

747 36. Andrews,A.E., Lawley,B. and Pittard,A.J. (1991) Mutational analysis of
748 repression and activation of the *tyrP* gene in *Escherichia coli*. *J. Bacteriol.*,
749 **173**, 5068–5078.

750 37. Leela,J.K., Syeda,A.H., Anupama,K. and Gowrishankar,J. (2013) Rho-
751 dependent transcription termination is essential to prevent excessive
752 genome-wide R-loops in *Escherichia coli*. *Proc. Natl. Acad. Sci. U. S. A.*, **110**,
753 258–263.

754 38. Amann,E., Ochs,B. and Abel,K.J. (1988) Tightly regulated *tac* promoter
755 vectors useful for the expression of unfused and fused proteins in
756 *Escherichia coli*. *Gene*, **69**, 301–315.

757 39. Datsenko,K.A. and Wanner,B.L. (2000) One-step inactivation of
758 chromosomal genes in *Escherichia coli* K-12 using PCR products. *Proc. Natl.*
759 *Acad. Sci. U. S. A.*, **97**, 6640–6645.

760 40. Sivaramakrishnan,P., Sepúlveda,L.A., Halliday,J.A., Liu,J., Núñez,M.A.B.,

761 Golding,I., Rosenberg,S.M. and Herman,C. (2017) The transcription fidelity
762 factor GreA impedes DNA break repair. *Nature*, **550**, 214–218.

763 41. Raghunathan,N., Goswami,S., Leela,J.K., Pandiyan,A. and Gowrishankar,J.
764 (2019) A new role for *Escherichia coli* Dam DNA methylase in prevention of
765 aberrant chromosomal replication. *Nucleic Acids Res.*, **47**, 5698–5711.

766 42. Gowrishankar,J. (1985) Identification of osmoresponsive genes in
767 *Escherichia coli*: Evidence for participation of potassium and proline
768 transport systems in osmoregulation. *J. Bacteriol.*, **164**, 434–445.

769 43. Raghunathan,N., Kapshikar,R.M., Leela,J.K., Mallikarjun,J., Bouloc,P. and
770 Gowrishankar,J. (2018) Genome-wide relationship between R-loop
771 formation and antisense transcription in *Escherichia coli*. *Nucleic Acids Res.*,
772 **46**, 3400–3411.

773 44. Azeroglu,B., Mawer,J.S.P., Cockram,C.A., White,M.A., Hasan,A.M.M.,
774 Filatenkova,M. and Leach,D.R.F. (2016) RecG directs DNA synthesis during
775 double-strand break repair. *PLoS Genet.*, **12**, e1005799.

776 45. White,M.A., Azeroglu,B., Lopez-Vernaza,M.A., Hasan,A.M.M. and
777 Leach,D.R.F. (2018) RecBCD coordinates repair of two ends at a DNA
778 double-strand break, preventing aberrant chromosome amplification.
779 *Nucleic Acids Res.*, **46**, 6670–6682.

780 46. Sambrook,J. and Russell,D. (2001) Molecular Cloning: A Laboratory Manual
781 3rd edn. Cold Spring Harbor Lab Press, New York.

782 47. Ali,N. and Gowrishankar,J. (2020) Cross-subunit catalysis and a new
783 phenomenon of recessive resurrection in *Escherichia coli* RNase E. *Nucleic*
784 *Acids Res.*, **48**, 847–861.

785 48. Boyd,D., Weiss,D.S., Chen,J.C. and Beckwith,J. (2000) Towards single-copy
786 gene expression systems making gene cloning physiologically relevant:
787 Lambda InCh, a simple *Escherichia coli* plasmid-chromosome shuttle
788 system. *J. Bacteriol.*, **182**, 842–847.

789 49. Konrad,E.B. (1977) Method for the isolation of *Escherichia coli* mutants with
790 enhanced recombination between chromosomal duplications. *J. Bacteriol.*,
791 **130**, 167–172.

792 50. Lovett,S.T., Hurley,R.L., Sutera,V.A., Aubuchon,R.H. and Lebedeva,M.A.
793 (2002) Crossing over between regions of limited homology in *Escherichia coli*:
794 RecA-dependent and RecA-independent pathways. *Genetics*, **160**, 851–859.

795 51. Dutra,B.E., Sutera,V.A. and Lovett,S.T. (2007) RecA-independent
796 recombination is efficient but limited by exonucleases. *Proc. Natl. Acad. Sci.*
797 *U. S. A.*, **104**, 216–221.

52. Lo´pez-Amoro´s,R., Comas,J. and Vives-Rego,J. (1995) Flow cytometric assessment of *Escherichia coli* and *Salmonella typhimurium* starvation survival in seawater using rhodamine 123, propidium iodide, and oxonol. *Appl. Environ. Microbiol.*, **61,** 2521-2526

53. Grylak-Mielnicka,A., Bidnenko,V., Bardowski,J. and Bidnenko,E. (2016) Transcription termination factor Rho: a hub linking diverse physiological processes in bacteria. *Microbiology*,**162**, 433-447.

54. Adhya,S. and Gottesman,M. (1978) Control of transcription termination. *Annu. Rev. Biochem.*, **47**, 967–996.

55. Gowrishankar,J. and Harinarayanan,R. (2004) Why is transcription coupled to translation in bacteria? *Mol. Microbiol.*, **54**, 598–603.

56. Peters,J.M., Mooney,R.A., Grass,J.A., Jessen,E.D., Tran,F. and Landick,R. (2012) Rho and NusG suppress pervasive antisense transcription in *Escherichia coli*. *Genes Dev.*, **26**, 2621–2633.

57. Harinarayanan,R. and Gowrishankar,J. (2003) Host factor titration by chromosomal R-loops as a mechanism for runaway plasmid replication in transcription termination-defective mutants of *Escherichia coli*. *J. Mol. Biol.*, **332**, 31–46.

58. Gowrishankar,J., Krishna Leela,J. and Anupama,K. (2013) R-loops in bacterial transcription: Their causes and consequences. *Transcription*, **4**, 153–157.

59. Washburn,R.S. and Gottesman,M.E. (2011) Transcription termination maintains chromosome integrity. *Proc. Natl. Acad. Sci. U. S. A.*, **108**, 792–797.

60. Johnson,D.B.F., Wang,C., Xu,J., Schultz,M.D., Schmitz,R.J., Ecker,J.R. and Wang,L. (2012) Release factor one is nonessential in *Escherichia coli*. *ACS Chem. Biol.*, **7**, 1337–1344.

61. Hu,K. and Artsimovitch,I. (2017) A screen for *rfaH* suppressors reveals a key role for a connector region of termination factor Rho. *mBio*, **8**, e00753-17.

62. Brandi,A., Piersimoni,L., Feto,N.A., Spurio,R., Alix,J.H., Schmidt,F. and Gualerzi,C.O. (2019) Translation initiation factor IF2 contributes to ribosome assembly and maturation during cold adaptation. *Nucleic Acids Res.*, **47**, 4652–4662.

63. Xia,J., Chen,L.T., Mei,Q., Ma,C.H., Halliday,J.A., Lin,H.Y., Magnan,D., Pribis,J.P., Fitzgerald,D.M., Hamilton,H.M., *et al.* (2016) Holliday junction trap shows how cells use recombination and a junction-guardian role of RecQ helicase. *Sci. Adv.*, **2**, e1601605.

64. Boguslawski,S.J., Smith,D.E., Michalak,M.A., Mickelson,K.E., Yehle,C.O., Patterson,W.L. and Carrico,R.J. (1986) Characterization of monoclonal antibody to DNA · RNA and its application to immunodetection of hybrids. *J. Immunol. Methods*, **89**, 123–130.

65. McGlynn,P. and Lloyd,R.G. (2000) Modulation of RNA polymerase by (p)ppGpp reveals a RecG-dependent mechanism for replication fork progression. *Cell*, **101**, 35–45.

66. Trautinger,B.W., Jaktaji,R.P., Rusakova,E. and Lloyd,R.G. (2005) RNA polymerase modulators and DNA repair activities resolve conflicts between DNA replication and transcription. *Mol. Cell*, **19**, 247–258.

67. Kamarthapu,V., Epshtein,V., Benjamin,B., Proshkin,S., Mironov,A., Cashel,M. and Nudler,E. (2016) ppGpp couples transcription to DNA repair in *E. coli*. *Science*, **352**, 993–996.

68. Carles-Kinch,K., George,J.W. and Kreuzer,K.N. (1997) Bacteriophage T4 UvsW protein is a helicase involved in recombination, repair and the regulation of DNA replication origins. *EMBO J.*, **16**, 4142–4151.

69. Dudas,K.C. and Kreuzer,K.N. (2001) UvsW protein regulates bacteriophage T4 origin-dependent replication by unwinding R-loops. *Mol. Cell. Biol.*, **21**, 2706–2715.

70. Magner,D.B., Blankschien,M.D., Lee,J.A., Pennington,J.M., Lupski,J.R.R. and Rosenberg,S.M. (2007) RecQ promotes toxic recombination in cells lacking recombination intermediate-removal proteins. *Mol. Cell*, **26**, 273–286.

71. Zhang,J., Mahdi,A.A., Briggs,G.S. and Lloyd,R.G. (2010) Promoting and avoiding recombination: Contrasting activities of the *Escherichia coli* RuvABC Holliday junction resolvase and RecG DNA translocase. *Genetics*, **185**, 23–37.

72. Florés,M.J., Sanchez,N. and Michel,B. (2005) A fork-clearing role for UvrD. *Mol. Microbiol.*, **57**, 1664–1675.

73. Capaldo,F.N. and Barbour,S.D. (1975) DNA content, synthesis and integrity in dividing and non-dividing cells of Rec$^-$ strains of *Escherichia coli* K12. *J. Mol. Biol.*, **91**, 53–66.

74. Miller,J.E. and Barbour,S.D. (1977) Metabolic characterization of the viable, residually dividing and nondividing cell classes of recombination deficient strains of *Escherichia coli*. *J. Bacteriol.*, **130**, 160–166.

75. Khodursky,A.B. and Cozzarelli,N.R. (1998) The mechanism of inhibition of topoisomerase IV by quinolone antibacterials. *J. Biol. Chem.*, **273**, 27668–27677.

873 76. Potrykus,K., Vinella,D., Murphy,H., Szalewska-Palasz,A., D'Ari,R. and
874 Cashel,M. (2006) Antagonistic regulation of *Escherichia coli* ribosomal RNA
875 *rrnB* P1 promoter activity by GreA and DksA. *J. Biol. Chem.*, **281**, 15238–
876 15248.

877 77. Vinella,D., Potrykus,K., Murphy,H. and Cashel,M. (2012) Effects on growth
878 by changes of the balance between GreA, GreB, and DksA suggest mutual
879 competition and functional redundancy in *Escherichia coli*. *J. Bacteriol.*, **194**,
880 261–273.

881 78. Gowrishankar,J. (2015) End of the beginning: Elongation and termination
882 features of alternative modes of chromosomal replication initiation in
883 bacteria. *PLoS Genet.*, **11**, e1004909.

884 79. Niu,Y., Tenney,K., Li,H. and Gimble,F.S. (2008) Engineering variants of the
885 I-SceI homing endonuclease with strand-specific and site-specific DNA-
886 nicking activity. *J. Mol. Biol.,* **382**, 188–202.

887 80. Laban,A. and Cohen,A. (1981) Interplasmidic and intraplasmidic
888 recombination in *Escherichia coli* K-12. *Mol. Gen. Genet.*, **184**, 200–207.

889 81. Cohen,A. and Laban,A. (1983) Plasmidic recombination in *Escherichia coli* K-
890 12: The role of *recF* gene function. *Mol. Gen. Genet.*, **189**, 471–474.

891 82. Zhang,G., Deng,E., Baugh,L. and Kushner,S.R. (1998) Identification and
892 characterization of *Escherichia coli* DNA helicase II mutants that exhibit
893 increased unwinding efficiency. *J. Bacteriol.*, **180**, 377-387.

894 83. Veaute,X., Delmas,S., Selva,M., Jeusset,J., Le Cam,E., Matic,I., Fabre,F. and
895 Petit,M.A. (2005) UvrD helicase, unlike Rep helicase, dismantles RecA
896 nucleoprotein filaments in *Escherichia coli*. *EMBO J.*, **24**, 180–189.

897 84. Nazir,A. and Harinarayanan,R. (2016) Inactivation of cell division protein
898 FtsZ by SulA makes Lon indispensable for the viability of a ppGpp^0 strain of
899 *Escherichia coli*. *J. Bacteriol.*, **198**, 688–700.

900 85. Ouyang,J., Yadav,T., Zhang,J.M., Yang,H., Rheinbay,E., Guo,H., Haber,D.A.,
901 Lan,L. and Zou,L. (2021) RNA transcripts stimulate homologous
902 recombination by forming DR-loops. *Nature*, **594**, 283-288.

903 86. Lesterlin,C., Ball,G., Schermelleh,L. and Sherratt,D.J. (2014) RecA bundles
904 mediate homology pairing between distant sisters during DNA break repair.
905 *Nature*, **506**, 249–253.

906 87. Centore,R.C. and Sandler,S.J. (2007) UvrD limits the number and intensities
907 of RecA-green fluorescent protein structures in *Escherichia coli* K-12. *J.*
908 *Bacteriol.*, **189**, 2915–2920.

909 88. Meddows,T.R., Savory,A.P., Grove,J.I., Moore,T. and Lloyd,R.G. (2005) RecN

protein and transcription factor DksA combine to promote faithful recombinational repair of DNA double-strand breaks. *Mol. Microbiol.*, **57**, 97–110.

89. Vickridge,E., Planchenault,C., Cockram,C., Junceda,I.G. and Espéli,O. (2017) Management of *E. coli* sister chromatid cohesion in response to genotoxic stress. *Nat. Commun.*, **8**, 14618.

90. Keyamura,K., Sakaguchi,C., Kubota,Y., Hironori,N. and Hishida,T. (2013) RecA protein recruits structural maintenance of chromosomes (SMC)-like RecN protein to DNA double-strand breaks. *J. Biol. Chem.*, **288**, 29229-29237.

91. Helleday,T., Lo,J., van Gent,D.C. and Engelward,B.P. (2007) DNA double-strand break repair: From mechanistic understanding to cancer treatment. *DNA Repair*, **6**, 923–935.

92. Chiruvella,K.K., Liang,Z. and Wilson,T.E. (2013) Repair of double-strand breaks by end joining. *Cold Spring Harb. Perspect. Biol.*, **5**, a012757.

93. Balestrini,A., Ristic,D., Dionne,I., Liu,X.Z., Wyman,C., Wellinger,R.J. and Petrini,J.H.J. (2013) The Ku heterodimer and the metabolism of single-ended DNA double-strand breaks. *Cell Rep.*, **3**, 2033-2045.

94. Ensminger,M. and Löbrich,M. (2020) One end to rule them all: Non-homologous end-joining and homologous recombination at DNA double-strand breaks. *Br. J. Radiol.*, **93**, 20191054.

95. Pham,N., Yan,Z., Yu,Y., Faria Afreen,M., Malkova,A., Haber,J.E. and Ira,G. (2021) Mechanisms restraining break-induced replication at two-ended DNA double-strand breaks. *EMBO J.*, **40**, e104847.

96. Badrinarayanan,A., Le,T.B.K., Spille,J.H., Cisse,I.I. and Laub,M.T. (2017) Global analysis of double-strand break processing reveals *in vivo* properties of the helicase-nuclease complex AddAB. *PLoS Genet.*, **13**, e1006783.

97. Kowalczykowski,S.C. (2015) An overview of the molecular mechanisms of recombinational DNA repair. *Cold Spring Harb. Perspect. Biol.*, **7**, a016410.

98. Krejci,L., Altmannova,V., Spirek,M. and Zhao,X. (2012) Homologous recombination and its regulation. *Nucleic Acids Res.*, **40**, 5795–5818.

99. Cox,M.M. (2007) Regulation of bacterial RecA protein function. *Crit. Rev. Biochem. Mol. Biol.*, **42**, 41–63.

100. Matic,I., Rayssiguier,C. and Radman,M. (1995) Interspecies gene exchange in bacteria: The role of SOS and mismatch repair systems in evolution of species. *Cell*, **80**, 507-515.

946 101. Renzette,N., Gumlaw,N. and Sandler,S.J. (2007) DinI and RecX modulate
947 RecA-DNA structures in *Escherichia coli* K-12.*Mol. Microbiol.*, **63**, 103-115.

948 102. Cohen,S.E., Lewis,C.A., Mooney,R.A., Kohanski,M.A., Collins,J.J.,
949 Landick,R. and Walker,G.C. (2010) Roles for the transcription elongation
950 factor NusA in both DNA repair and damage tolerance pathways in
951 *Escherichia coli*. *Proc. Natl. Acad. Sci. U. S. A.*, **107**, 15517–15522.

952 103. Cohen,S.E. and Walker,G.C. (2010) The transcription elongation factor
953 NusA is required for stress-induced mutagenesis in *Escherichia coli*. *Curr.*
954 *Biol.*, **20**, 80–85.

955 104. Epshtein,V., Kamarthapu,V., McGary,K., Svetlov,V., Ueberheide,B.,
956 Proshkin,S., Mironov,A. and Nudler,E. (2014) UvrD facilitates DNA repair by
957 pulling RNA polymerase backwards. *Nature*, **505**, 372–377.

958 105. Shazand,K., Tucker,J., Chiang,R., Stansmore,K., Sperling-Petersen,H.U.,
959 Grunberg-Manago,M., Rabinowitz,J.C. and Leighton,T. (1990) Isolation and
960 molecular genetic characterization of the *Bacillus subtilis* gene (*infB*)
961 encoding protein synthesis initiation factor 2. *J. Bacteriol.*, **172**, 2675–2687.

962

Legends to figures

Figure 1: Synthetic lethality of *rho ruv* and of *uvrD ruv* mutants, and their suppression by loss of IF2-1 or by *rec* mutations. Unless otherwise indicated, designations *rho* and *ruv* that are not further qualified refer to alleles *rho*-136^{opal} and Δ*ruvABC*::Cm, respectively. All strain numbers mentioned are prefixed with GJ. (A) Blue-white screening assays, on defined medium at 30°, for strains carrying *rho*$^{+}$ *infB*$^{+}$ shelter plasmid pHYD5212. Representative images are shown; for each of the sub-panels, relevant chromosomal genotypes/features are given on top while the numbers beneath indicate the percentage of white colonies to total (minimum of 500 colonies counted). Examples of white colonies are marked by yellow arrows. Growth medium for sub-panels vii, viii, and xi was supplemented with IPTG. Strains employed for the different sub-panels were pHYD5212 derivatives of: i, 15441; ii, 15447; iii, 15446; iv, 15498; v, 15500; vi, 15499; vii, 15458; viii, 15457; ix, 19134; x, 19131; and xi, 19132. (B) Dilution-spotting assay, on minimal A supplemented with Glu or Ara as indicated, of *rho*-136^{opal} strains bearing P$_{ara}$-*rho*$^{+}$; other relevant genotypes/features are shown at left. Strains for different rows were (from top): 1, 19379; 2, 19380; 3, 19381 (this strain was grown in Ara-supplemented medium before dilutions were spotted); and 4, 19382. (C) Blue-white screening assays to determine whether *rec* or *lexA3* mutations suppress *rho ruv* synthetic lethality. Methods used, and notations, are similar to those in panel A. A Δ*ruvA* allele was used for sub-panel vi. Strains employed were pHYD5212 derivatives of: i, 15460; ii, 15471; iii, 15491; iv, 15487; v, 15497; and vi, 15485. (D) Dilution-spotting assay, on LB medium without (−) and with (+) Dox supplementation, of RDG-bearing derivatives whose relevant genotypes/features are indicated at left; strains on all but the top two rows were also Δ*infB*. Strains employed for different rows were (from top): 1, 19127; 2, 19161; 3, 19801; 4, 19802; 5, 19803; 6, 19843; and 7, 19835.

Figure 2: Loss of IF2-1 is associated with sensitivity to two-ended DSBs in DNA. In all panels, strains designated Δ*Nil*, Δ*1*, or Δ*2,3* were also Δ*infB*, as too was the *recA* strain in panel B. (A-B) Dilution-spotting assays, on LB medium with

supplements as indicated on top (Phleo and Bleo each at 0.5 µg/ml, Glu and Ara each at 0.2%), of different strains whose relevant genotypes/features are marked. (C) Flow cytometry following propidium iodide staining of cells in LB-grown cultures of strains whose relevant genotypes/features are indicated on top and perturbations, if any, at left; Phleo supplementation was at 2 µg/ml, and I-SceI refers to Ara-supplementation in cultures of derivatives carrying P_{ara}::I-SceI and the cognate cut site in *lacZ*. In each sub-panel, the percentage of total cells whose intensity of propidium iodide staining exceeded the threshold that was taken to demarcate dead cells (3 x 10^3 arbitrary units, marked by vertical line), is indicated at top right. Strains employed across all three panels were (all strain numbers mentioned are prefixed with GJ): I. derivatives without P_{ara}::I-SceI – Δ*Nil*, 19193; Δ*2,3*, 19194; Δ*1*, 15494; *recA*, 19844; *priB*, 19812; and *priA300,* 15495; and II. derivatives with P_{ara}::I-SceI – *infB*$^+$, 15837; Δ*Nil*, 19804; Δ*2,3*, 19805; Δ*1*, 19806; and *recA*, 19818.

Figure 3: Chromosomal DNA copy number analysis by WGS following two-ended DSB generation at *lacZ*. DNA copy numbers (after normalization) are plotted as semi-log graphs for overlapping 10-kb intervals across the genome for derivatives each carrying P_{ara}::I-SceI and the cognate cut site in *lacZ*, after supplementation of cultures grown in LB with 0.2% Glu (control) or Ara for 1 hr (top and bottom rows, respectively). Relevant genotypes/features are indicated within each of the panels; all strains were also Δ*infB*. In these Cartesian graphical representations, the circular 4642-kb long chromosome is shown linearized at *oriC*, with genome coordinates on the abscissa corresponding to the MG1655 reference sequence (wherein *oriC* is at 3926 kb). Ordinate scales (log_2) shown at left on top and bottom rows are common for, respectively, panels i-iv and v-vii. The positions of *lacZ, TerA* and *TerC/B* are marked. Strains used were (all strain numbers mentioned are prefixed with GJ): Δ*Nil*, 19804; Δ*2,3*, 19805; Δ*1*, 19806; and *recA*, 19818.

Figure 4: Effect of IF2 isoforms on HR. Recombination frequency data are given for strains with the indicated genotypes/features in the Konrad (A), inter-plasmid

recombination (B), and P1 transduction (C) assays, after normalization to the value for the cognate control strain (taken as 1, and shown at extreme left for each panel); the actual control strain values were $2.8*10^{-7}$/viable cell, $6*10^{-4}$/viable cell, and $1.5*10^{-5}$/phage, respectively. In panels A and B, values from every individual experiment is shown, and median values are given beside the denoted horizontal lines. Panel C depicts the mean value (given alongside each bar) and standard error for each strain. In all panels, strains whose designations include Δ*Nil*, Δ*1*, or Δ*2,3* were also Δ*infB*. Strains used were (from left, all strain numbers mentioned are prefixed with GJ unless otherwise indicated): in panel A, SK707, 19171, 19186, 19162, 19184, and 19165; in panel B, 19197, 19196, 19195, and 19847; and in panel C, 19193, 19194, and 15494.

Fig. 1

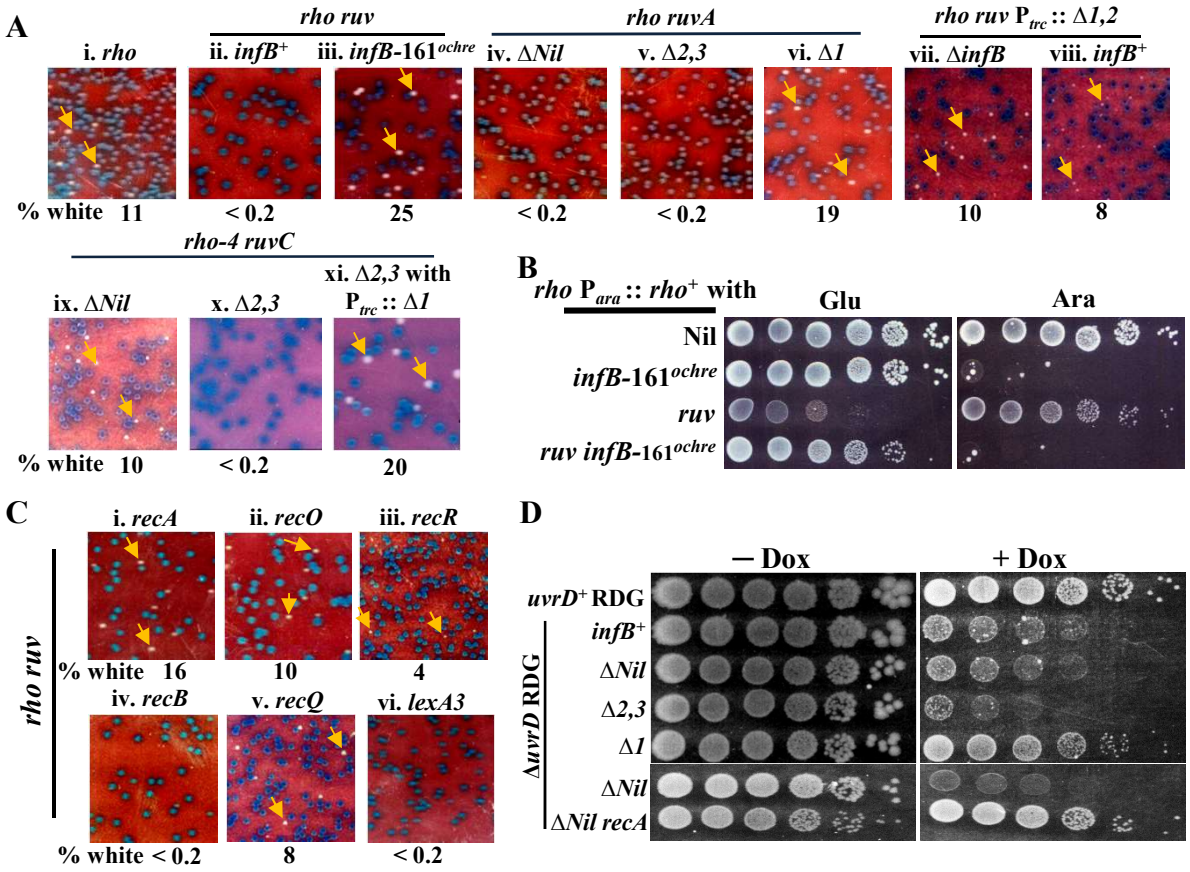

Figure 1: Synthetic lethality of *rho ruv* and of *uvrD ruv* mutants, and their suppression by loss of IF2-1 or by *rec* mutations. Unless otherwise indicated, designations *rho* and *ruv* that are not further qualified refer to alleles *rho*-136^{opal} and Δ*ruvABC*::Cm, respectively. All strain numbers mentioned are prefixed with GJ. (A) Blue-white screening assays, on defined medium at 30°, for strains carrying *rho*$^{+}$ *infB*$^{+}$ shelter plasmid pHYD5212. Representative images are shown; for each of the sub-panels, relevant chromosomal genotypes/features are given on top while the numbers beneath indicate the percentage of white colonies to total (minimum of 500 colonies counted). Examples of white colonies are marked by yellow arrows. Growth medium for sub-panels vii, viii, and xi was supplemented with IPTG. Strains employed for the different sub-panels were pHYD5212 derivatives of: i, 15441; ii, 15447; iii, 15446; iv, 15498; v, 15500; vi, 15499; vii, 15458; viii, 15457; ix, 19134; x, 19131; and xi, 19132. (B) Dilution-spotting assay, on minimal A supplemented with Glu or Ara as indicated, of *rho*-136^{opal} strains bearing P$_{ara}$-*rho*$^{+}$; other relevant genotypes/features are shown at left. Strains for different rows were (from top): 1, 19379; 2, 19380; 3, 19381 (this strain was grown in Ara-supplemented medium before dilutions were spotted); and 4, 19382. (C) Blue-white screening assays to determine whether *rec* or *lexA3* mutations suppress *rho ruv* synthetic lethality. Methods used, and notations, are similar to those in panel A. A Δ*ruvA* allele was used for sub-panel vi. Strains employed were pHYD5212 derivatives of: i, 15460; ii, 15471; iii, 15491; iv, 15487; v, 15497; and vi, 15485. (D) Dilution-spotting assay, on LB medium without (−) and with (+) Dox supplementation, of RDG-bearing derivatives whose relevant genotypes/features are indicated at left; strains on all but the top two rows were also Δ*infB*. Strains employed for different rows were (from top): 1, 19127; 2, 19161; 3, 19801; 4, 19802; 5, 19803; 6, 19843; and 7, 19835.

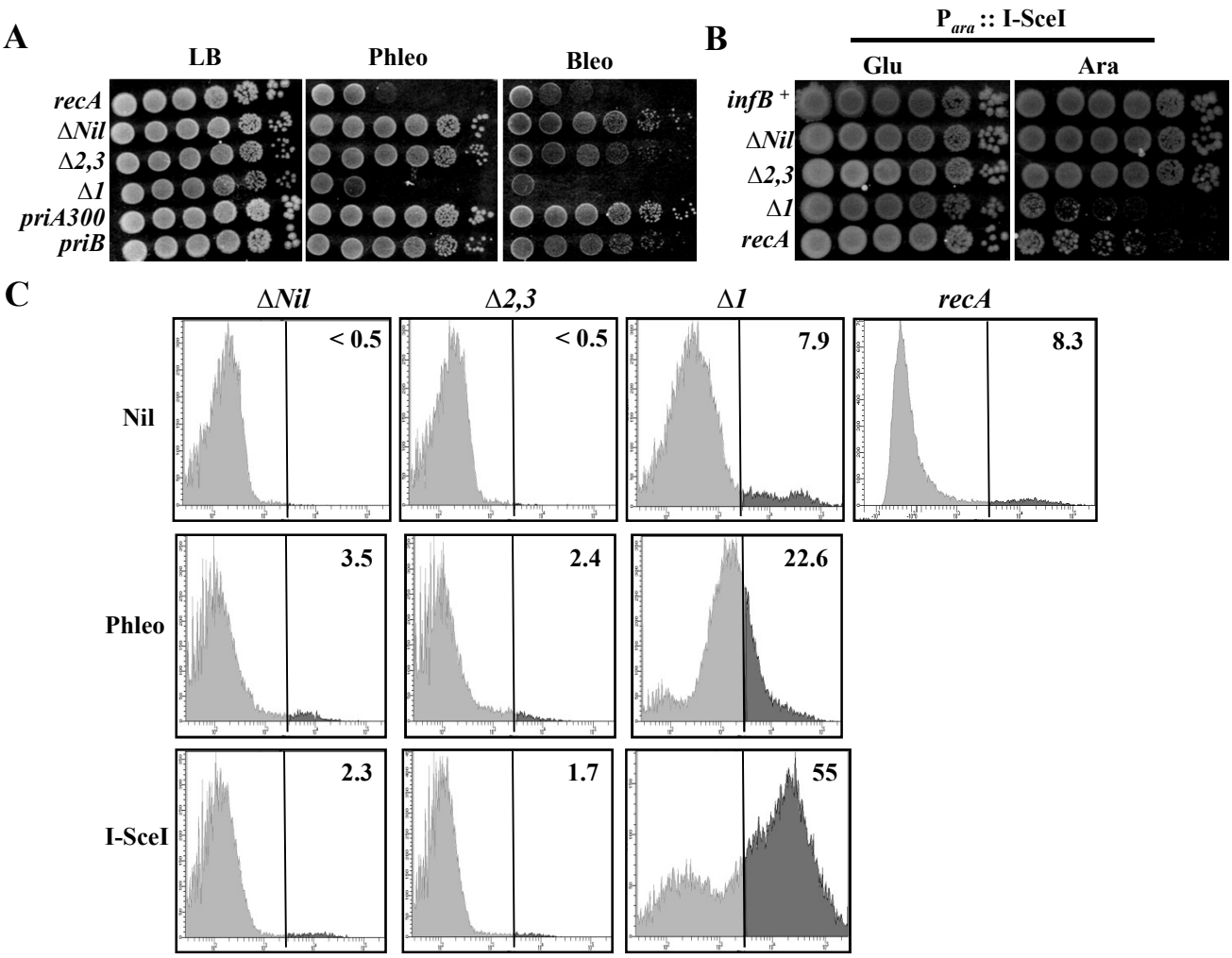

Figure 2: Loss of IF2-1 is associated with sensitivity to two-ended DSBs in DNA. In all panels, strains designated Δ*Nil*, Δ*1*, or Δ*2,3* were also Δ*infB*, as too was the *recA* strain in panel B. (A-B) Dilution-spotting assays, on LB medium with supplements as indicated on top (Phleo and Bleo each at 0.5 μg/ml, Glu and Ara each at 0.2%), of different strains whose relevant genotypes/features are marked. (C) Flow cytometry following propidium iodide staining of cells in LB-grown cultures of strains whose relevant genotypes/features are indicated on top and perturbations, if any, at left; Phleo supplementation was at 2 μg/ml, and I-SceI refers to Ara-supplementation in cultures of derivatives carrying P_{ara}::I-SceI and the cognate cut site in *lacZ*. In each sub-panel, the percentage of total cells whose intensity of propidium iodide staining exceeded the threshold that was taken to demarcate dead cells (3 x 10^3 arbitrary units, marked by vertical line), is indicated at top right. Strains employed across all three panels were (all strain numbers mentioned are prefixed with GJ): I. derivatives without P_{ara}::I-SceI – Δ*Nil*, 19193; Δ*2,3*, 19194; Δ*1*, 15494; *recA*, 19844; *priB*, 19812; and *priA300,* 15495; and II. derivatives with P_{ara}::I-SceI – *infB*$^+$, 15837; Δ*Nil*, 19804; Δ*2,3*, 19805; Δ*1*, 19806; and *recA*, 19818.

Fig. 3

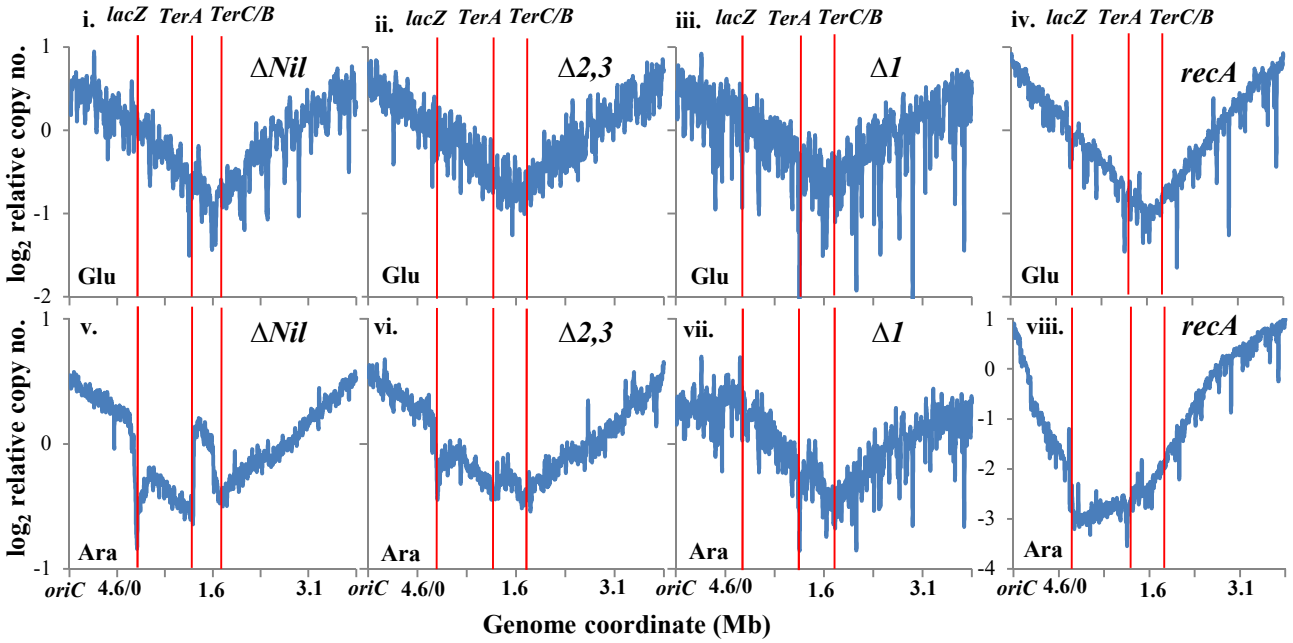

Figure 3: Chromosomal DNA copy number analysis by WGS following two-ended DSB generation at *lacZ*. DNA copy numbers (after normalization) are plotted as semi-log graphs for overlapping 10-kb intervals across the genome for derivatives each carrying P_{ara}::I-SceI and the cognate cut site in *lacZ*, after supplementation of cultures grown in LB with 0.2% Glu (control) or Ara for 1 hr (top and bottom rows, respectively). Relevant genotypes/features are indicated within each of the panels; all strains were also Δ*infB*. In these Cartesian graphical representations, the circular 4642-kb long chromosome is shown linearized at *oriC*, with genome coordinates on the abscissa corresponding to the MG1655 reference sequence (wherein *oriC* is at 3926 kb). Ordinate scales (log_2) shown at left on top and bottom rows are common for, respectively, panels i-iv and v-vii. The positions of *lacZ, TerA* and *TerC/B* are marked. Strains used were (all strain numbers mentioned are prefixed with GJ): Δ*Nil*, 19804; Δ*2,3*, 19805; Δ*1*, 19806; and *recA*, 19818.

Fig. 4

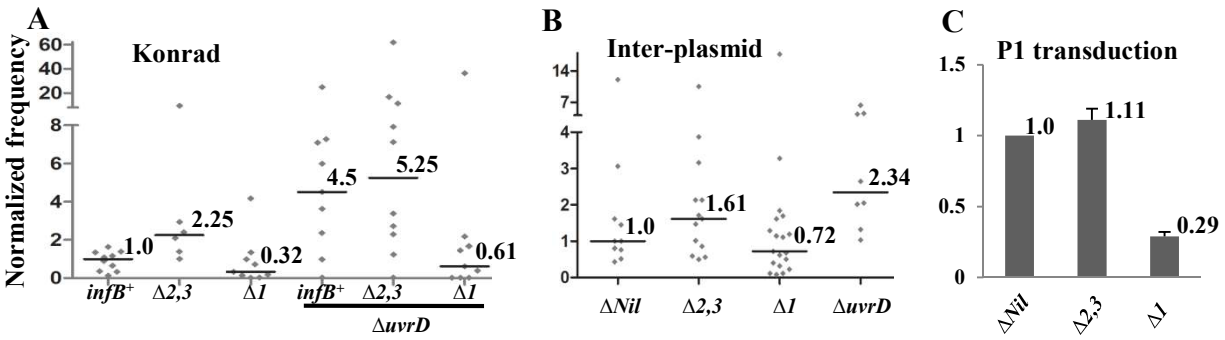

Figure 4: Effect of IF2 isoforms on HR. Recombination frequency data are given for strains with the indicated genotypes/features in the Konrad (A), inter-plasmid recombination (B), and P1 transduction (C) assays, after normalization to the value for the cognate control strain (taken as 1, and shown at extreme left for each panel); the actual control strain values were $2.8*10^{-7}$/viable cell, $6*10^{-4}$/viable cell, and $1.5*10^{-5}$/phage, respectively. In panels A and B, values from every individual experiment is shown, and median values are given beside the denoted horizontal lines. Panel C depicts the mean value (given alongside each bar) and standard error for each strain. In all panels, strains whose designations include Δ*Nil*, Δ*1*, or Δ*2,3* were also Δ*infB*. Strains used were (from left, all strain numbers mentioned are prefixed with GJ unless otherwise indicated): in panel A, SK707, 19171, 19186, 19162, 19184, and 19165; in panel B, 19197, 19196, 19195, and 19847; and in panel C, 19193, 19194, and 15494.